JOURNAL OF NANO- AND ELECTRONIC PHYSICS
Vol. **11** No 4, 04009(3pp) (2019)

ЖУРНАЛ НАНО- ТА ЕЛЕКТРОННОЇ ФІЗИКИ
Том **11** № 4, 04009(3cc) (2019)

Watershed Segmentation Image Processing Analysis of $Zn_{0.97}Fe_{0.03}O$ Dilute Magnetic Semiconductor

Vishal Mathur[1,*], Rana Mukherji[2]

[1] *Sur University College, Sur, Oman*
[2] *The ICFAI University, Jaipur, India*

(Received 09 April 2019; revised manuscript received 01 August 2019; published online 22 August 2019)

The particle size distribution is a fundamental parameter for describing the fabric and features of the specimens. It is also important for a better understanding of their dynamic behavior. Segmentation of a digital image is the method of dissection into various disjoint sections, so that pixels of each section have alike visual features. This concept is used to determine particle size distribution through image analysis. Watershed image processing analysis is one of the prevalent methods for image segmentation. In accordance to this algorithm, a grayscale image is transformed into a topographic image that consists of various diverse basins just like regions that are flooded with water, in which different watersheds lines are apportioning similar particle size regions. In the present work, the watershed algorithm is developed using MATLAB and applied to scanning electron microscopy (SEM) image to assess the nanoparticles distribution of dilute magnetic semiconductor specimen of zinc oxide (ZnO) doped with Fe (at 3 % molar concentration). The specimen is prepared through a solid-state reaction technique and then vacuum-annealed at ~ 1000 °C approximately for 48 hours. The SEM image of $Zn_{0.97}Fe_{0.03}O$ directly reveals that the grains of ZnO altered their floret-like shape into hexagonal prism-like shape upon Fe doping. Watershed image processing analysis reveals that the blended particles of ZnO and Fe retain their adequate nanosize and fine distribution for the studied specimen.

Keywords: MATLAB, Watershed algorithm, Scanning electron microscopy, Diluted magnetic semiconductors, ZnO.

DOI: 10.21272/jnep.11(4).04009 PACS numbers: 85.75.d, 75.50.Pp, 75.50.Bb, 77.84.Bw

1. INTRODUCTION

Diluted magnetic semiconductors (DMSs) based on wide-gap oxide semiconductor systems, such as SnO_2, ZnO, TiO_2, In_2O_3, etc. doped with transition metal (Cr, Co, Mn, Fe, Co, Ni, etc.) have received a prodigious attention in current technical communal for offering room temperature ferromagnetism (RTFM) property [1-6]. The oxide DMSs are sensitive towards limiting light and offer dye potentiality with pigments. They exhibit adequate transparency and high n-type carrier concentration [7].

Sato and Katayama-Yoshida [10] are among the first who theoretically investigated ferromagnetism (FM) in TM-doped ZnO through local density approximation (LDA) based on ab-initio calculations. Duan et al. [11] revealed that the enrichment of both the magnetization and the intensity of Raman scattering peak allied with donor defects and carriers specifies that light $Zn_{1-x}Cr_xO$ could be an effective way to attain noticeable RTFM. They also suggested that FM is meticulously associated to the dopant-donor hybridization besides the Cr–O–Cr superexchange interactions. Kundaliya et al. [12] observed RTFM for 2 wt. % Mn-ZnO bulk specimen, but there is a little bit of confusion over the mechanism behind the ferromagnetism, as it may be due to Mn_2O_3 phase or due to some other phase. To check the reproducibility, Garcia et al. [13] also followed the same preparation technique and observed that aggrandizing the sintering temperature above 600 °C resulted in a diminution of RTFM and its complete vanishing after sintering at 800 °C. They concluded that the presence of both Mn^{3+} and Mn^{4+} is accountable for FM through the double-exchange mechanism. Liu et al. [14] showed that FM of the Ni-doped ZnO nanoparticles is originated from the presence of the Vo (oxygen vacancy). They also depicted that the saturated magnetization firstly increases and then decreases with the increase of Ni concentration, which results from the competition between oxygen vacancies and antiferromagnetic coupling between Ni^{2+} in NiO. Wojnarowicz et al. [15] blended ZnO-Co by the typical microwave solvothermal synthesis route. They investigated a relationship between local structures, valence of the Co atoms and that in turn the valence stoutly clouts the prominent carrier type with magnetism in the Zn-Co-O system. Yu et al. [16] used homogeneous precipitation method to prepare Fe-doped and Co-co-doped ZnO specimens. They also found a hexagonal wurtzite structure and an ancillary phase of spinel in doped ZnO. Wang et al. [17] studied bulk specimens of $Zn_{1-x}Fe_xO$ (x = 0-3 %) series prepared by a co-precipitation method. All the specimens showed FM at room temperature. The results of XRD showed that the specimens ($x \leq 2$ %) were of single phase, while a secondary phase $ZnFe_2O_4$ was observed in $x = 3$ % specimen. However, the formation of secondary phase $ZnFe_2O_4$ did not result in a crucial effect on the magnetic moment. Shukla et al. [18] studied the optical and sensing properties of undoped and $Zn_{1-x}Fe_xO$ films that had been successfully deposited by spray pyrolysis method. They revealed that doping with Fe increased the transmission of the films as the dopant concentration steadily increased for both molarities. Dinesha et al. [19] used solution combustion method to

* wishalmathur@gmail.com

synthesize $Zn_{1-x}Fe_xO$ (where $x = 0.00$, 0.005, 0.01, 0.02, 0.03, 0.04) and studied the dielectric and structural behavior of specimens. They proposed the diminution in dielectric parameters with increase of Fe doping. Saleh et al. [20] depicted a diminution in the energy gap with upsurge in Fe concentration whereas Mishra and Das [21] also witnessed a decrease in particle size with upsurge in the Fe contents.

The literature reveals that most of the studies of TM-doped ZnO are focused on the findings of structural and RTFM properties. In view of analysis of structural properties, scanning electron microscopy (SEM) is among the very frequently used techniques, but it is not so much discussed in detail anywhere in the available literature. The present paper is focused on SEM image analysis of $Zn_{0.97}Fe_{0.03}O$ through MATLAB based watershed image processing technique. The study reveals that the blended particles of ZnO and Fe retain their adequate nano-dimension and fine distribution for the studied specimen.

2. MATERIALS AND METHODS

2.1 Specimen Preparation

The $Zn_{0.97}Fe_{0.03}O$ DMS specimen is prepared by doping Fe at 3 % molar concentration into ZnO matrix through solid-state reaction technique [22-24] and vacuum annealed at ~ 1000 °C for approximately 48 h. SEM observation is taken through NOVA NANO FE-SEM 450 (FEI) SEM model. MATLAB-based simulation is carried out to investigate the homogeneity in particle distribution within $Zn_{0.97}Fe_{0.03}O$ through SEM micrograph.

2.2 Watershed Algorithm

As known, particle size distribution is a fundamental parameter for describing the fabric and features of the specimens. MATLAB based image processing analysis based on the watershed algorithm is used to evaluate the homogeneity particle distribution through SEM images of DMSs specimens. The algorithm is developed by Luc Vincent and Pierre Soille [25]. According to the algorithm, every local minimum of a greyscale image can be observed as a surface has a hole and the surface is submerged into water. Subsequently, beginning from the minima of lowermost intensity value, the water will gradually fill up diverse catchment basins of image. The method is also important for a better understanding of their dynamic behavior.

3. IMAGE ANALYSIS

The SEM image of $Zn_{0.97}Fe_{0.03}O$ (Fig. 1) directly reveals that the grains of ZnO altered their floret-like shape into hexagonal prism-like shape upon Fe doping. MATLAB based watershed segmentation algorithm [25, 26], which is a more intuitive image processing analysis tool, is used to evaluate the analogousness particle distribution through SEM image. In this algorithm, firstly distance transform tool is applied on the binary SEM micrograph image that engenders a distance map in terms of variation in pixel brightness.

After that, topological surface image is created through this distance map in a successive step. In the final image, bright pixels correspond to profound parts of the constitute ZnO and Fe of $Zn_{0.97}Fe_{0.03}O$ DMS specimen. In this image, a basin is formed for each blended ZnO and Fe segment irrespective of their type, tagged with random color for distinct vision. The final image is governed with a particle size distribution curve with respect to their relative intensity that also shows that the specimen bears nanocharacteristic structurally. The segmented map and

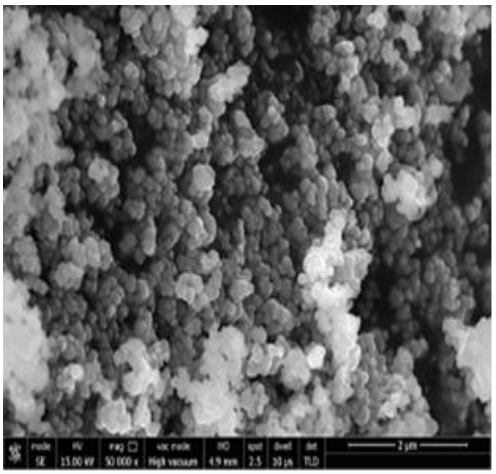

Fig. 1 – SEM image of $Zn_{0.97}Fe_{0.03}O$

Fig. 2 – Watershed segmental plot of $Zn_{0.97}Fe_{0.03}O$

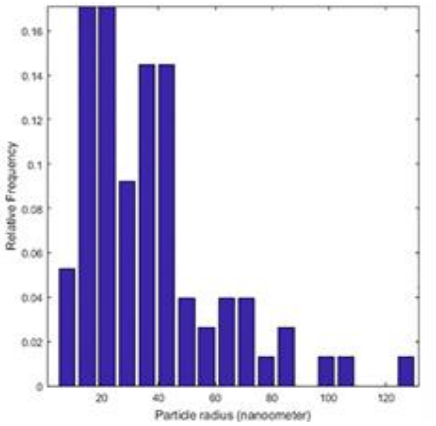

Fig. 3 – Particle size distribution curve of $Zn_{0.97}Fe_{0.03}O$

particle size distribution curve of $Zn_{0.97}Fe_{0.03}O$ DMS specimen are as shown in Fig. 2 and Fig. 3. The result also shows that the average particle size is 37.5627 nm of constituting ZnO and Fe ions in the studied sample.

4. CONCLUSIONS

The SEM image of $Zn_{0.97}Fe_{0.03}O$ clearly reveals that the grains of ZnO transform their floret-like shape into hexagonal prism-like shape upon Fe doping. MATLAB based watershed segmentation algorithm is successfully employed on SEM micrograph of $Zn_{0.97}Fe_{0.03}O$ specimen. This watershed image processing analysis reveals that the blended particles of ZnO and Fe create basins of similar particle size. The average particle size is observed as 37.5627 nm, which is better for understanding the dynamic behavior of $Zn_{0.97}Fe_{0.03}O$.

REFERENCES

1. R. Elilarassi, G. Chandrasekaran, *Spectrochim Acta A* **186**, 120 (2017).
2. G.S. Shanker, B. Tandon, T. Shibata, S. Chattopadhyay, A. Nag, *Chem. Mater.* **27**, 892 (2015).
3. B.U. Haq, R. Ahmed, A. Shaari, N. Ali, Y. Al-Douri, A.H. Reshak, *Mat. Sci. Semicon. Proc.* **43**, 123 (2016).
4. S.L. Ou, H.R. Liu, S.Y. Wang, D.S. Wuu, *J. Alloy. Compd.* **663**, 107 (2016).
5. S. Zaineb, S. Atiq, A. Mahmood, S.M. Ramay, S. Riaz, S. Naseem, *J. Mater. Sci-Mater. El.* **29**, 3943 (2018).
6. H. Ohno, *Science* **281**, 951 (1998).
7. H. Ohno, *Phys. Rev.* **68**, 2664 (1992).
8. T.E. Mølholt, H.P. Gunnlaugsson, K. Johnston, R. Mantovan, J. Röder, V. Adoons, A.M. Gerami, H. Masenda, Y.A. Matveyev, M. Ncube, I. Unzueta, *J. Phys.: Condens. Matter.* **29**, 155701 (2017).
9. R. Mukherji, V. Mathur, A. Samariya, M. Mukherji, *J. Adv. Nanomater.* **2**, 105 (2017).
10. K. Sato, H. Katayama-Yoshida, *Jpn. J. Appl. Phys.* **39**, L555 (2000).
11. L.B. Duan, X.R. Zhao, J.M. Liu, T. Wang, G.H. Rao, *Appl. Phys. A* **99**, 679 (2010).
12. D.C. Kundaliya, S.B. Ogale, S.E. Lofland, S. Dhar, C.J. Metting, S.R. Shinde, Z. Ma, B. Varughese, K.V. Ramanujachary, L. Salamanca-Riba, T. Venkatesan, *Nat. Mater.* **3**, 709 (2004).
13. M.A. García, M.L. Ruiz-González, A. Quesada, J.L. Costa-Krämer, J.F. Fernández, S.J. Khatib, A. Wennberg, A.C. Caballero, M.S. Martín-González, M. Villegas, F. Briones, *Phys. Rev. Lett.* **94**, 217206 (2005).
14. Y. Liu, H. Liu, Z. Chen, N. Kadasala, C. Mao, Y.Y. Zhang, H. Liu, Y. Liu, J. Yang, Y. Yan, *J Alloy. Compd.* **604**, 281 (2014).
15. J. Wojnarowicz, S. Kusnieruk, T. Chudoba, S. Gierlotka, W. Lojkowski, W. Knoff, T. Story, *Beilstein J. Nanotechnol.* **6**, 1957 (2015).
16. X. Yu, D. Meng, C. Liu, X. He, Y. Wang, J. Xie, *Mater. Lett.* **86**, 112 (2012).
17. Y.Q. Wang, S.L. Yuan, L. Liu, P. Li, X.X. Lan, Z.M. Tian, J.H. He, S.Y. Yin, *J. Magn. Magn. Mater*, **320**, 1423 (2008).
18. R.K. Shukla, A. Srivastava, N. Kumar, A. Pandey, M. Pandey, *Mater. Sci-Poland* **34**, 354 (2016).
19. M.L. Dinesha, G.D. Prasanna, C.S. Naveen, H.S. Jayanna, *Indian J. Phys.* **87**, 147 (2013).
20. R. Saleh, S.P. Prakoso, A. Fishli, *J. Magn. Magn. Mater.* **324**, 665 (2012).
21. A.K. Mishra, D. Das, *Mater. Sci. Eng. B* **171**, 5 (2010).
22. R.K. Singhal, A. Samariya, Y.T. Xing, S. Kumar, S.N. Dolia, U.P. Deshpande, T. Shripathi, E.B. Saitovitch *J. Alloy. Compd.* **496**, 324 (2010).
23. R. Mukherji, V. Mathur, A. Samariya, M. Mukherji, *J. Nano-Electron. Phys.* **9**, 02003 (2017).
24. R. Mukherji, V. Mathur, M. Mukherji, *J. Nano- Electron. Phys.* **10**, 05008 (2018).
25. A. Rabbani, S. Ayatollahi, *Special Topics & Reviews in Porous Media: An International Journal* **6**, 71 (2015).
26. R. Mukherji, V. Mathur, A. Samariya, M. Mukherji, *Adv. Compos. Hybrid Mater.* **1**, 809 (2018).

Сегментний аналіз обробки зображень за морфологічними вододілами розбавленого магнітного напівпровідника $Zn_{0.97}Fe_{0.03}O$

Vishal Mathur[1], Rana Mukherji[2]

[1] *Sur University College, Sur, Oman*
[2] *The ICFAI University, Jaipur, India*

Розподіл частинок за розміром є фундаментальним параметром для опису матеріалів і особливостей зразків. Це також важливо для кращого розуміння їх динамічної поведінки. Сегментація цифрового зображення є методом розшарування в різні роздільні ділянки так, що пікселі кожної секції мають однакові візуальні особливості. Ця концепція використовується для визначення розподілу частинок за розміром за допомогою аналізу зображень. Аналіз обробки вододільних зображень є одним з поширених методів сегментації зображень. Відповідно до цього алгоритму, зображення у градаціях сірого перетворюється на топографічне зображення, яке складається з різноманітних басейнів, подібно до регіонів, які затоплені водою, в яких різні лінії вододілів розподіляють області частинок подібних розмірів. У даній роботі алгоритм вододілу розроблений з використанням MATLAB і застосований до зображень скануючої електронної мікроскопії (SEM) для оцінки розподілу наночастинок розбавленого магнітного напівпровідникового зразка оксиду цинку (ZnO), легованого Fe (при 3 % молярній концентрації). Зразок готують методом твердофазної реакції і потім вакуумно відпалюють при ~ 1000 °C приблизно протягом 48 годин. SEM зображення $Zn_{0.97}Fe_{0.03}O$ безпосередньо свідчить про те, що зерна ZnO змінювали свою подібну до квітки форму на гексагональну призмоподібну форму після легування Fe. Аналіз обробки вододільних зображень показує, що змішані частинки ZnO і Fe зберігають свій адекватний нанорозмір і точний розподіл для досліджуваного зразка.

Ключові слова: MATLAB, Алгоритм вододілів, Скануюча електронна мікроскопія, Розбавлені магнітні напівпровідники, ZnO.